

# 3D-Cell-Annotator technical details

## 1 Introduction

In this supplementary, we introduce the theoretical foundations for the methods used in the software. 3D-Cell-Annotator is based on an extended version of active contours called selective active contour model [1]. The selective active contour model introduces two different priors, the *volume* and the *shape* prior; these priors are proposed in 3D-Cell-Annotator to extract single cells from clusters. Two different data terms are tested, the first one is the simplest *anisotropic edge detector* while the other one, called the *local region* data term, considers the environment of the contour to find the boundary of the object more effectively. The implementation uses the level set framework that naturally handles the topological deformations of the contour. Since one of the most fundamental limitations of the level set method is its numerical instability, we proposed a new method called *balanced phase field model*, that regularizes the level set in a *narrow band* in every iteration step to achieve numerical stability during the segmentation [2]. We briefly discuss both models here since these are the main building blocks of the algorithm used by the proposed software.

## 2 Selective active contours in 3D

The 2D selective active contour model was introduced to segment objects by considering their size and shape [1, 3]. We chose the level set framework because it is a powerful method for implementing interfacial problems like active contours [4].

### 2.1 Notations

Surfaces are denoted by  $\mathbf{S} \subseteq \mathbb{R}^3$  or  $\mathbf{S}(u, v) \in \mathbb{R}^3$  in parameterized form, where  $u$  and  $v$  are surface parameters.  $\mathbf{S}_u(u, v), \mathbf{S}_v(u, v) \in \mathbb{R}^3$  are partial derivatives wrt. surface parameters  $(u, v)$ , providing local (covariant) basis for the vectors of the tangent plane at  $\mathbf{S}(u, v)$ . Recall that  $\mathbf{S}_u \times \mathbf{S}_v$  is normal to the surface. Assuming  $\mathbf{S}_u, \mathbf{S}_v, \mathbf{n}$  constitute a right handed basis, the inward pointing unit normal  $\frac{\mathbf{S}_u \times \mathbf{S}_v}{|\mathbf{S}_u \times \mathbf{S}_v|}$  is denoted by  $\mathbf{n}$ . The sum curvature of the surface is denoted by  $K$ , while  $K_G$  is the Gaussian curvature. The integral  $\int dS = \int \sqrt{|\mathbf{S}_u|^2 |\mathbf{S}_v|^2 - (\mathbf{S}_u \cdot \mathbf{S}_v)^2} dudv$  gives the surface area and  $\int dV = -\frac{1}{6} \int \mathbf{S} \cdot (\mathbf{S}_u \times \mathbf{S}_v) dudv$  gives the volume of a surface  $\mathbf{S}$ , where  $dS$  and  $dV$  are the surface and volume element respectively.

Level set functions are denoted by  $\phi = \phi(t, \mathbf{x})$ , where  $t \in \mathbb{R}$  and  $\mathbf{x} = (x_1, x_2, x_3) \in \mathbb{R}^3$  are the time and space variables, respectively. According to this,  $\phi_t$  denotes the partial derivative with respect to the time and  $\nabla\phi$  denotes the spatial gradient  $\nabla\phi = (\phi_{x_1}, \phi_{x_2}, \phi_{x_3})$ . The Hessian matrix of  $\phi$  is denoted by  $\mathbf{H}(\phi) = (\phi_{x_i x_j})_{1 \leq i, j \leq 3}$ .

## 2.2 The selective functional

There are four terms included in the functional of the selective active contour model. Below we provide a concise summary. For the details, see the original paper [1].

### 2.2.1 Volume prior

The volume prior prefers objects having a certain size and it is denoted by  $V_0$ .

$$\mathcal{V}(\mathbf{S}) = \frac{1}{kV_0^k} \left( \int dV - V_0 \right)^k \quad (1)$$

The  $k$  is an arbitrary integer. If it is 2 then the contour tries to have a volume of exactly  $V_0$  while if it is 3, it has an inflection at  $V_0$  therefore it prefers a volume of 0 except at  $V_0$  where the term has no effect.

### 2.2.2 Shape prior

The shape prior penalizes the deviation of the current surface from the preferred shape  $p$  (*plasma* or *amoeba value*). The currently implemented shape prior is called *sphericity* in 3D-Cell-Annotator but essentially it is the surface/volume ratio of the surface that is calculated as  $p = \frac{\text{area}^{\frac{3}{2}}}{\text{volume}}$ . The plasma value is minimal for the sphere, that is  $p = 3\sqrt{4\pi} \approx 10.6$ . We normalize the prior to assign 1.0 to the sphere so the sphericity is given by  $p - 9.6$ .

The shape prior that considers the surface volume ratio is then:

$$\mathcal{S}(\mathbf{S}) = \frac{1}{2V_0^2} \left[ \left( \int dS \right)^{\frac{3}{2}} - p \int dV \right]^2 \quad (2)$$

### 2.2.3 Smoothness term

A curvature based smoothness term is applied to prevent the instability of the surface called Euler elastica. For the details, consult the original paper [1].

$$\mathcal{E}(\mathbf{S}) = \frac{1}{2} \int K^2 dS, \quad (3)$$

where the  $K$  is the sum curvature of the surface at a given point.

### 2.2.4 Data term

Two different data terms are tested, but there is a wide range of possible ones to choose from. The first one is the simple edge detector:

$$\mathcal{D}_{\mathcal{E}}(\mathbf{S}) = \int \nabla I \cdot \mathbf{n} dS, \quad (4)$$

where the  $I$  is the image.

The second one is a region based data term. It considers the mean intensities in the rectangular prisms positioned both in the inner and the outer side of the surface. In our setting the functional maximizes the intensity difference between the inner and outer part. If this data term is used, then the algorithm has three more parameters that define the size of the region (width, height and depth).

$$\Phi(\mathbf{S}, \mathbf{n}) = \frac{1}{4pqr} \left( \int_{\mathfrak{R}^+} I(\mathbf{p}) dV - \int_{\mathfrak{R}^-} I(\mathbf{p}) dV \right), \quad (5)$$

where  $dV = d\xi d\zeta d\eta$ ,  $\xi \in [-p, p]$ ,  $\zeta \in [-q, q]$  and  $\eta \in [0, r]$ .  $\mathbf{p}$  is in the local coordinate system, therefore  $\mathbf{p} = \mathbf{S} + \xi \mathbf{e}_1 + \zeta \mathbf{e}_2 + \eta \mathbf{n}$  as it is visualised in fig. (1).

Therefore, we can use the local region as a data term in the selective model:

$$\mathcal{D}_{\mathcal{R}}(\mathbf{S}) = \int \Phi(\mathbf{S}, \mathbf{n}) dS. \quad (6)$$

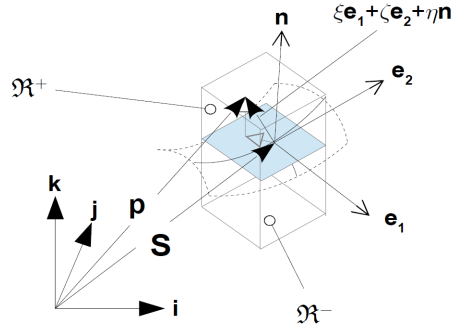


Figure 1: Visualisation of the local region in 3D. The local Cartesian coordinate system of the region is centered at the surface point  $\mathbf{S}$  while the orientation is determined by the unit normal vector of the surface  $\mathbf{n}$  and the unit basis vectors  $\mathbf{e}_1, \mathbf{e}_2$  of the tangential plane of the surface.

### 2.2.5 Putting it all together: the composite functional

The composite functional therefore consists of the previously introduced terms and becomes the following:

$$\mathcal{L} = \alpha\mathcal{D} + \beta\mathcal{S} + \gamma\mathcal{V} + \delta\mathcal{E}, \quad (7)$$

where each term has an arbitrary real weight that can be controlled from the interface of the 3D-Cell-Annotator. The  $\mathcal{D}$  can be either  $\mathcal{D}_\mathcal{E}$  or  $\mathcal{D}_\mathcal{R}$  depending on which data term is used.

### 2.3 The Euler-Lagrange equation for the functional

The extremal surface of the functional above can be found by solving the corresponding Euler-Lagrange equations. In our case (3D surfaces in the level set framework) they have the form:

$$|\mathbf{S}_u \times \mathbf{S}_v|Q\mathbf{n} = \mathbf{0}, \quad (8)$$

where  $Q$  is a scalar field with the functional derivatives:  $Q = \alpha Q_{\mathcal{D}_\mathcal{E}} + \beta Q_{\mathcal{S}} + \gamma Q_{\mathcal{V}} + \delta Q_{\mathcal{E}}$ .

That is, for the volume prior, we have  $Q_{\mathcal{V}} = -\frac{1}{V_0^3}(\int dV - V_0)^2$  ( $V_0$  is the target volume), for the shape prior (that takes sphericity into consideration)  $Q_{\mathcal{S}} = \left[ \left( \int dS \right)^{\frac{3}{2}} - p \int dV \right] \left[ p - \frac{3}{2}K \left( \int dS \right)^{\frac{1}{2}} \right]$ ,  $p$  is the (unnormalized) target plasma value ( $p = \frac{\text{surface}^{\frac{3}{2}}}{\text{volume}}$ ), for the data term, we have  $Q_{\mathcal{D}_\mathcal{E}} = \Delta I$  and for the smoothness term we have  $Q_{\mathcal{E}} = \frac{1}{2}K^3 - 2K_G K + \nabla \cdot \nabla K$ , where  $K_G$  is the Gaussian curvature. The Euler-Lagrange of  $\mathcal{D}_\mathcal{R}$  is slightly more complicated [3].

## 3 Level set regularization: the Balanced Phase Field model

### 3.1 Notations

In the level set framework, the representation of contours is given by a level set function of two variables  $\phi(x, y)$ . The quantities of the segmentation problem are extracted from this function, such as the unit normal vector  $\mathbf{n} = \frac{\nabla\phi}{|\nabla\phi|}$  or the curvature  $K = -\nabla \cdot \left( \frac{\nabla\phi}{|\nabla\phi|} \right)$  where  $\nabla$  is the gradient operator and “ $\cdot$ ” stands for the scalar (dot) product, *i.e.*  $\nabla \cdot \mathbf{v}$  is the divergence of the vector field  $\mathbf{v}$ .

### 3.2 From the phase field model to the balanced model

Since one of the fundamental problems of the level set method is its numerical instability, one should take care about the numerical errors by using some regularization method explicitly by not letting the active contour model to deform the level set from the signed distance function too much. We experienced severe issues with our selective model when we computed the curve evolution in level set framework, and the tested approximate solutions did not solve the issue,

while the more accurate methods made the algorithm too slow to be practical in reality. A simple observation is that maintaining the whole level set during the evolution is not necessary, since we always consider the derivatives in the neighborhood of the interface. Therefore it is enough to maintain the stability in this neighborhood called narrow band. Therefore we chose to apply a modified phase field solution to regularize the level set in every iteration. Using such a model, we treat the level set as a phase field, where the inner part of the contour is encoded with value 1 while the outer is with  $-1$ . Between the two, there is a *phase transition* with a necessary zero-crossing that models the contour. The goal is to maintain a smooth phase transition that is similar to the signed distance property of the level set near the contour. Furthermore, using the modified phase field model called balanced phase field, the authors do not only propose a solution to the numerical issues of the level sets but also eliminate the effect of the regularization method on the active model. In the following, we discuss the most important aspects of the model for the two dimensional case starting from the original phase field model and introducing the ideas behind the improved balanced phase field. For the details, and the intermediate steps of the derivation, consult [2].

In the original functional we had:

$$\int \int_{\Omega} \frac{D_0}{2} |\nabla \phi|^2 + \lambda_0 \left( \frac{\phi^4}{4} - \frac{\phi^2}{2} \right) dA. \quad (9)$$

The solution of (9) is a scalar field  $\phi$  with values  $\pm 1$  and a phase transition between the two values representing the narrow band of the contour. It is possible to embed the functional (9) to the active contour model directly by extending its functional with it, however it may lead to an extremely complex system considering its analysis. Instead of applying the phase field directly, one can use it in a shape maintenance role: before the next evolution step, the Euler-Lagrange equation associated with (9) can be solved independently, providing a regularized narrow band to the next iteration step.

However, a careful analysis shows that applying this functional to the level sets has a serious side effect on the active model by producing a curvature driven motion. In order to fix this issue, a Laplacian smoothness term is introduced and the original functional becomes the following:

$$\int \int_{\Omega} \frac{D}{2} (\Delta \phi)^2 + \lambda \left( \frac{\phi^4}{4} - \frac{\phi^2}{2} + \frac{1}{4} \right) dA. \quad (10)$$

However the proposed functional (10) still has a curvature dependent term and therefore produces the same effect when applied. It was shown that by using the combination of the smoothness terms from the previous functionals in a new one, with appropriate choice of the relative weights, the curvature dependency can be almost fully eliminated [2]. The new functional then becomes the following:

$$\int \int_{\Omega} \frac{D}{2} |\Delta \phi|^2 - \frac{D_0}{2} |\nabla \phi|^2 + \lambda \left( \frac{\phi^4}{4} - \frac{\phi^2}{2} + \frac{1}{4} \right) dA. \quad (11)$$

The conditions needed to be satisfied in order to cancel the effect of the curvature in the functional (11) depend on the width of the phase transition ( $w$ ):

$$\lambda w^4 - 24D_0 w^2 - 720D = 0, \quad (12)$$

and

$$-D_0 \frac{3}{w} + D \frac{48}{w^3} = 0. \quad (13)$$

In order to satisfy the conditions (12) and (13), one should compute the parameters of (11) as a function of the desired width of the phase transition. Therefore we first should determine the width of the phase transition needed. This depends on the highest order of derivatives ( $n$ ) used in the active model since we have to consider at least  $n + 1$  points around the contour if we use the central difference schemes. The phase transition is non-linear, but the deviation from the linearity of its innermost part is negligible. This near-linear part is confined to the immediate neighbors of zero level set with the extent about half the size of the width parameter. Therefore, assuming the  $n$ -neighbors are used to calculate the differential quantities of the contour (using finite differences scheme) we use width parameter  $2n+1$  to obtain accurate values. Then, solving the conditions above, for the remaining parameters we get:

$$D_0 = 1, D = \frac{w^2}{16}, \lambda = \frac{21}{w^2}. \quad (14)$$

The associated Euler-Lagrange functional with the parameters only depending on the width of the phase transition is:

$$\frac{w^2}{16} \Delta \Delta \phi + \Delta \phi + \frac{21}{w^2} (\phi^3 - \phi) = 0. \quad (15)$$

The (15) can be implemented as simply as applying a (4-th order linear) filter modified by a point-wise value of the nonlinear (cubic) term for the grid points of the phase field lattice.

## 4 Implementation details

We briefly discuss the implementation of the selective algorithm and the 3D-Cell-Annotator software.

### 4.1 The selective model with the balanced phase field reinitialization model

We solve the Euler-Lagrange equations in the level set framework, therefore the following quantities can be substituted:

$$\mathbf{S}_u \times \mathbf{S}_v \mapsto \nabla\phi, \quad \mathbf{n} \mapsto \frac{\nabla\phi}{|\nabla\phi|}, \quad (16)$$

while the curvatures are computed as:

$$K \mapsto -\nabla \cdot \frac{\nabla\phi}{|\nabla\phi|}, \quad K_G \mapsto |\nabla\phi|^{-4} \begin{vmatrix} \mathbf{H}(\phi) & \nabla\phi^T \\ \nabla\phi & 0 \end{vmatrix}. \quad (17)$$

For minimizing the functionals a simple gradient descent is used. The finite differences are used to compute the derivatives numerically.

## 4.2 The software

The selective model is targeted to the CUDA architecture in C++. The level set values are only computed where the surface is located in the current iteration. The algorithm is distributed as a shared library and a new tool is created in the MITK that implements the communication between the shared library and the MITK.

## References

- [1] J. Molnar, E. Tasnadi, B. Kintszes, Z. Farkas, C. Pal, P. Horvath, and T. Danka. Active surfaces for selective object segmentation in 3d. In *2017 International Conference on Digital Image Computing: Techniques and Applications (DICTA)*, pages 1–7, Nov 2017.
- [2] J. Molnar, E. Tasnadi, and P. Horvath. A balanced phase field model for active contours. In *Seventh International Conference on Scale Space and Variational Methods in Computer Vision (SSVM 2019)*, pages 1–7, 2019.
- [3] J. Molnar, A. I. Szucs, C. Molnar, and P. Horvath. Active contours for selective object segmentation. In *2016 IEEE Winter Conference on Applications of Computer Vision (WACV)*, pages 1–9, March 2016.
- [4] S. Osher and J. Sethian. Fronts Propagating With Curvature Dependent Speed: Algorithms Based on Hamilton-Jacobi Formulations. *Journal of Computational Physics*, 79(1):12–49, 1988.